

Search for cosmic-ray antideuterons with BESS-Polar

K. YOSHIMURA¹ K. ABE,^{2,a} H. FUKU,³ S. HAINO,^{1,b} T. HAMS,^{4,c} M. HASEGAWA,¹ A. HORIKOSHI,¹ K. C. KIM,⁵ A. KUSUMOTO,² M. H. LEE,⁵ Y. MAKIDA,¹ S. MATSUDA,¹ Y. MATSUKAWA,² J. W. MITCHELL,⁴ J. NISHIMURA,⁶ M. NOZAKI,¹ R. ORITO,^{2,d} J. F. ORMES,⁷ K. SAKAI,^{6,e} M. SASAKI,^{4,f} E. S. SEO,⁵ R. SHINODA,⁶ R. E. STREITMATTER,⁴ J. SUZUKI,¹ K. TANAKA,¹ N. THAKUR,⁷ T. YAMAGAMI,³ A. YAMAMOTO,^{1,6} AND T. YOSHIDA,³

¹High Energy Accelerator Research Organization (KEK), Tsukuba, Ibaraki 305-0801, Japan

²Kobe University, Kobe, Hyogo 657-8501, Japan

³Institute of Space and Astronautical Science, Japan Aerospace Exploration Agency (ISAS/JAXA), Sagami-hara, Kanagawa 252-5210, Japan

⁴National Aeronautics and Space Administration, Goddard Space Flight Center (NASA/GSFC), Greenbelt, MD 20771, USA

⁵IPST, University of Maryland, College Park, MD 20742, USA

⁶The University of Tokyo, Bunkyo, Tokyo 113-0033, Japan

⁷University of Denver, Denver, CO 80208, USA

koji.yoshimura@kek.jp

Abstract: Although cosmic-ray antideuterons can be produced in primary cosmic-ray interactions with the interstellar medium in the same way as cosmic-ray antiprotons, the probability is much smaller, especially at low energies, because of the very low production cross-section and strict kinematic requirement compared to secondary antiproton production. The lack of significant astrophysical background indicates that a search for low-energy antideuterons could be a good probe for a novel production mechanisms such as pair-annihilation of neutralino dark matter or evaporation of primordial black holes. The BESS-Polar program has accumulated cosmic-ray data in near solar minimum conditions with more than ten times the statistics of those obtained by BESS flights during the previous solar minimum period. Based on these data, we perform a new antideuteron search with unprecedented sensitivity.

Keywords: BESS-Polar, Antideuteron, Long-duration balloon flight, Solar minimum

1 Introduction

Cosmic-ray antiprotons (\bar{p} 's) have been unique probe to investigate elementary particle phenomena in the early universe and to study fundamental cosmic-ray processes, e.g. production, propagation, and solar modulation. This is primarily because most of \bar{p} 's are produced in primary cosmic-ray interactions with the interstellar medium (so-called "secondary \bar{p} 's") and the flux can be well-predicted by various theoretical models. [1, 2, 3, 4, 5]. Novel primary origins, if they exist, would exhibit themselves as flux enhancement over the secondary antiproton spectrum. Many experimental programs have been measuring \bar{p} 's and pursuing their origins. The data from BESS '95 and '97 taken in the last solar minimum period showed flatter \bar{p} spectrum towards low energy, which might suggest the existence of a primary origin[6]. Data reported recently from both PAMELA and BESS-Polar II[7, 8], however, showed good consistency with secondary \bar{p} 's.

Cosmic-ray antideuterons (\bar{d} 's) are in a different situation. Thanks to their heavier mass, the probability of production in cosmic-ray interaction is much smaller, especially at low energies, because of the very low production cross-section and strict kinematical requirement. So one single \bar{d} event would be a direct evidence of novel primary origins[9, 10] However, expected flux is extremely small and numerous \bar{p} 's become severe background to identify \bar{d} 's. An experiment with large exposure factor and good particle identification devices is necessary to investigate \bar{d} 's. As such, few searches have been carried out so far and no \bar{d} candidate was observed yet. The best limit was reported by the BESS experiment obtained during last solar minimum period[11].

a. Present address: ICRR, Tokyo

b. Present address: INFN, Perugia

c. Also at: CRESST/University of MD Baltimore County

d. Present address: Tokushima University

e. Also at: CRESST/University of MD College Park

f. Present address: NASA/GSFC

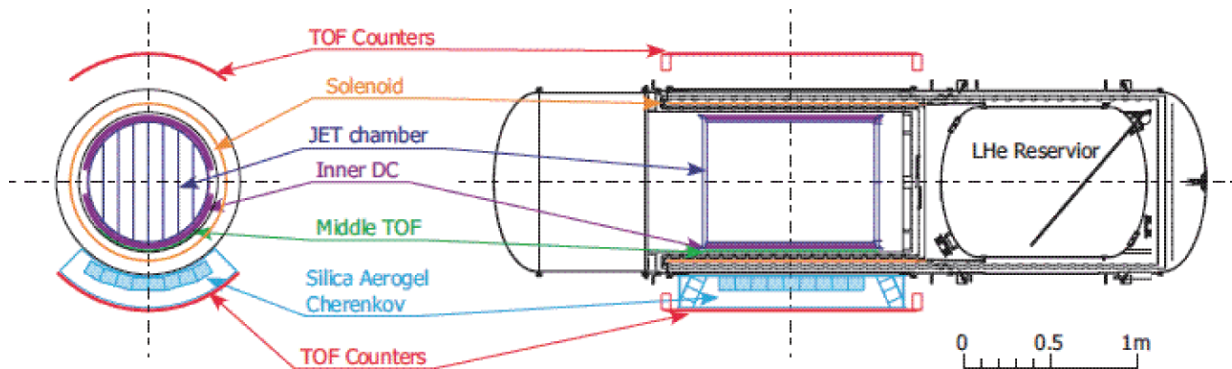


Figure 1: Cross sectional view of BESS-Polar II instrument.

There are several on-going and future program which could further investigate \bar{d} 's [12, 13, 14]. BESS-Polar II, second long duration flight over antarctica, was carried out in 2007/8 and data analysis is proceeded. The data taken during 24.5 scientific observation provide a good opportunity to search for \bar{d} especially in the low energy region since the flight was performed in the solar minimum period as well as entirely in the low geomagnetic cutoff region. We could expect great improvement over the last reported data from the BESS experiment. In this paper, current status on analysis to search for \bar{d} will be described.

2 BESS-Polar II Instrument and Flight

BESS-Polar II, the second flight of BESS-Polar, had been prepared to be carried out at the solar minimum with an improved instrument and capability for an extended long-duration flight. We expected a 20 day flight with two circumnavigation over Antarctica to gather cosmic-ray events with 20 times more statistics than BESS97 flight. To meet the requirements we had newly-built the BESS-Polar II instrument [15, 16].

Figure 1 shows a cross-sectional view of the BESS-Polar II instrument. A uniform field of 0.8 T is produced by a thin superconducting solenoid, and the field region is filled with tracking detectors. Cylindrical coaxial geometry realize a large acceptance of $0.23 \text{ m}^2\text{sr}$. Tracking is performed by fitting up to 48 hit points in drift chambers (JET) and 4 hit points in inner drift chambers (IDC), resulting in a magnetic-rigidity ($R \equiv Pc/Ze$) resolution of 0.4% at 1 GV, and a maximum detectable rigidity (MDR) of 270 GV. The upper and lower scintillator hodoscopes provide time-of-flight (TOF) and dE/dx measurements as well as trigger signal. The timing resolution of each hodoscope is 120 ps, resulting in a β^{-1} resolution of 3.3%. The instrument also incorporates a threshold-type Cherenkov counter with a silica aerogel radiator with refractive index $n = 1.03$ (ACC) that can reject e^- and μ^- backgrounds by a factor of 6000. The threshold rigidities for \bar{p} (p) and \bar{d} (d) are 3.8 GV and 7.6 GV, respectively. In addition, a thin scintillator middle-TOF (MTOF) is installed between the central tracker and

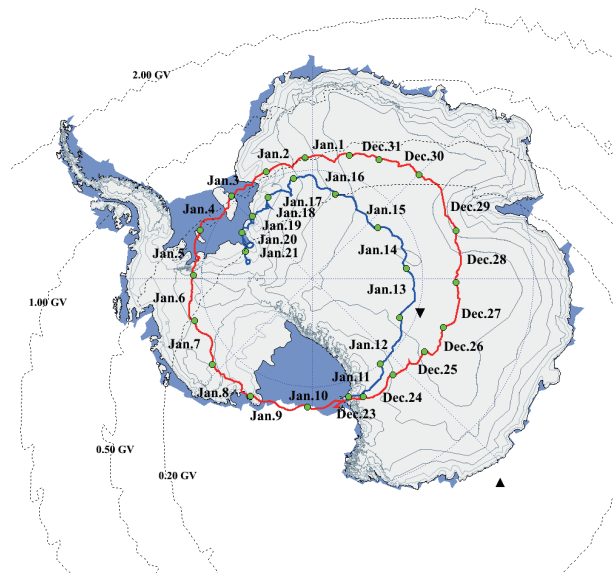
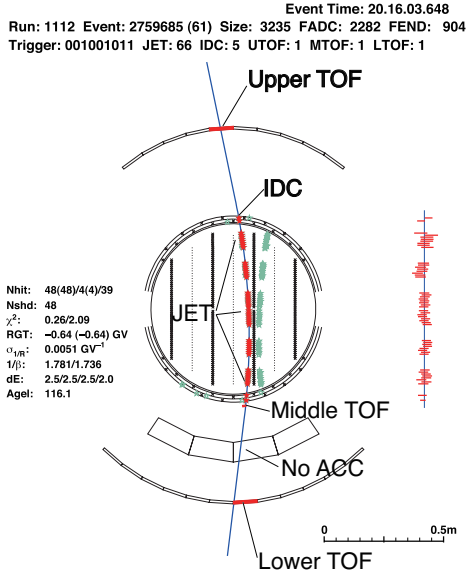


Figure 2: BESS-Polar II Flight trajectory. Contour lines indicate geomagnetic cutoff rigidity.

the solenoid to detect low energy particles which cannot penetrate the magnet wall. The timing resolution of these hodoscopes is 320 ps.

The BESS-Polar II flight was carried out in December 2007 through January 2008. The payload was launched on December 23 from Williams Field near the US McMurdo Station in Antarctica and circulated around the South Pole for 29.5 days as shown in Figure 2. Data were taken for live-time periods of 1286460 seconds at altitudes of 34 km to 38 km (residual air of 5.8 g/cm^2 on average). The cutoff rigidity was kept under 0.6 GV for the entire flight trajectory. 4.7×10^9 cosmic-ray events were accumulated without any online event selections as 13.6 terabytes of data recorded in the hard disk drives. During the 24.5 days of observation, all detectors operated well and they exhibited the expected performance except for the central tracker. The JET chamber showed an instability due to high-voltage fluctuation. However more than 90% of the data has been successfully calibrated while keeping sufficient tracker quality, a task that was realized by development of time-dependent tracker calibration.

Figure 3: Event display of one of \bar{p} candidate

3 Data Analysis

Data analysis on \bar{d} is similar to that used for antiproton measurements as described in [17]. First, clean single track events which pass through the fiducial region are selected as shown in Figure 3. Then we use a combination of the information from particle identification devices to extract \bar{d} (d) signals. Antiprotons are now major backgrounds to be separated from \bar{d} 's. At this point, the same selection criteria for positive and negative curvature events are applied under the assumption that non-interactive \bar{d} (\bar{p}) behave like d (p) except for their deflection thanks to the cylindrical symmetry of the BESS-Polar spectrometer. We can also estimate various efficiencies for \bar{d} 's by using positive curvature events (d).

3.1 Event selection

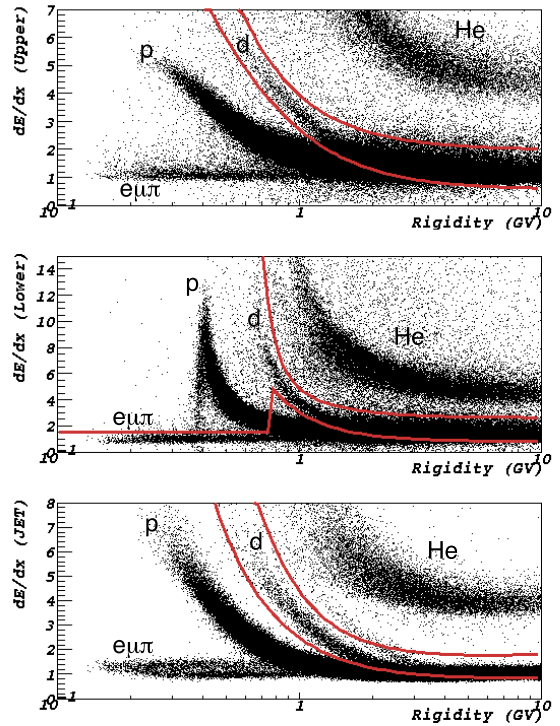
To select clean high-quality single track events which provide reliable information for further analysis, the following two stages of the selections are applied:

pre-selection

Select non-interacting particles which pass through the fiducial region by using JET number-of-hit information, the TOF number of hits, Track position, etc. The surviving events are used for starting samples to be used for later analysis.

track quality cut

The various cuts are then applied to ensure the quality of the track along with correct timing information by using χ^2 of the track fitting, consistency between track and TOF hit information, number of z -hit information from IDC, etc. These cuts also eliminate hard scattered events.

Figure 4: dE/dx vs rigidity plots for upper TOF (top), lower TOF (middle), and JET chamber (bottom), respectively. The curves in each plot define dE/dx band cut position.

3.2 Deuteron and Antideuteron identification

d and \bar{d} candidates are then selected by using combination of dE/dx , ACC and β information.

We first apply band selections according to dE/dx for upper and lower TOF and JET chamber. Figure 4 shows dE/dx vs. rigidity plot for each detector. We require that \bar{d} 's as well as d 's must have the dE/dx inside the " dE/dx " band shown in Figure 4. In the low rigidity region, this dE/dx cut rejects most of $e/\mu/\pi$, p and \bar{p} , and all of the particles with charge greater than 1.

The ACC veto cut is then applied to reject relativistic $e/\mu/\pi$ samples as well as p 's and \bar{p} 's having rigidity higher than threshold ($E > 3.8$ GV).

Figure 5 shows the scatter plot of β^{-1} vs. rigidity before and after the dE/dx and the ACC cut. In the top plot, clear band structures are visible, each of which corresponds to particle mass as $m = R\sqrt{1/\beta^2 - 1}$. By applying the dE/dx cut, most of the particles are eliminated except for the d (\bar{d}) and relativistic particle ($e/\mu/\pi/p$). In the bottom plot, further rejection was done by the ACC veto. Now we can clearly extract d (\bar{d}) signals. The curves are shown define a 3σ band from the center of the β^{-1} distribution for d samples. The close-up view of the rectangular area between 1.5 to 5 GV are shown in the top-right corner. The remaining background of p 's (\bar{p} 's) fall within the 3σ area for rigidities between 2 ~ 4.5 GV. We eliminate these from the \bar{d} signal region.

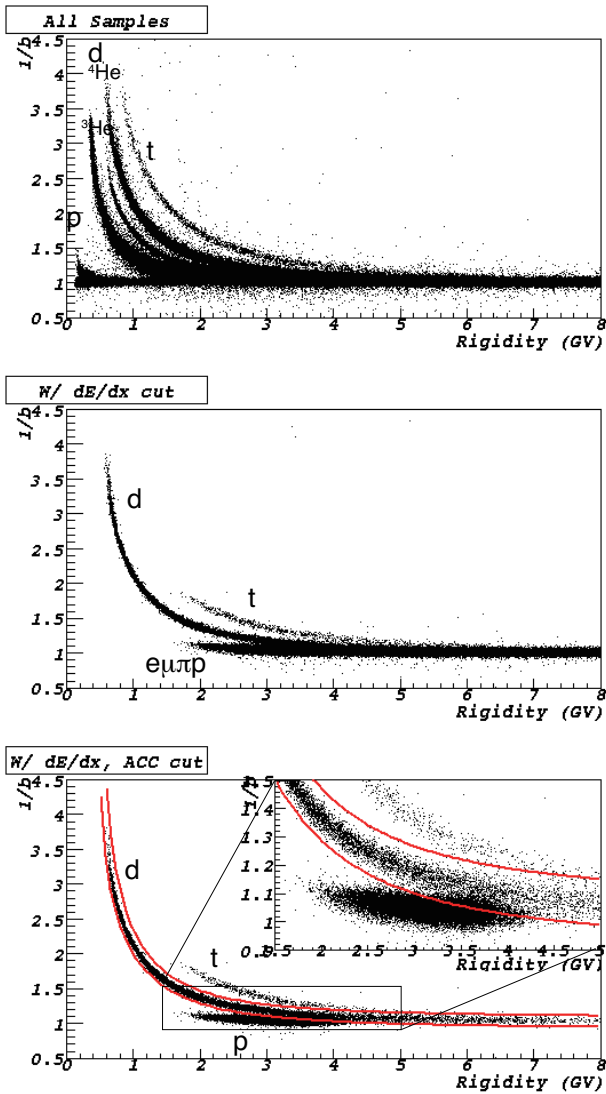


Figure 5: β^{-1} vs. rigidity plot. The top plot is for the samples before the dE/dx and the ACC cut. The middle and the bottom plots are for the samples after the dE/dx cut, and both dE/dx and the ACC veto cut, respectively.

4 Summary

Now we are carefully estimating background contamination in the signal region by using control samples while optimizing selection criteria and signal region so that the expected number of background is less than one. We also study efficiency by using both MC and real data samples. In the conference, we will report the result about \bar{d} search based on the BESS-Polar II data.

Acknowledgements

The authors thank NASA Headquarters for the continuous encouragement in this U.S.-Japan cooperative project. Sincere thanks are expressed to the NASA Balloon Programs

Office at GSFC/WFF and CSBF for their experienced support. They also thank ISAS/JAXA and KEK for their continuous support and encouragement. Special thanks go to the National Science Foundation (NSF), U.S.A., and Raytheon Polar Service Company for their professional support in U.S.A. and in Antarctica. The BESS-Polar experiment is being carried out as a Japan-U.S. collaboration, and is supported by a KAKENHI(13001004,18104006, and 22540322) in Japan, and by NASA in U.S.A.

References

- [1] T. Mitsui, Ph.D. thesis, the University of Tokyo (1996).
- [2] J. W. Bieber *et al.*, Phys. Rev. Lett. **83**, 674 (1999); Proc. 26th Int. Cosmic Ray Conf. (Utah) **7**, 17 (1999).
- [3] L. Bergström *et al.*, Astrophys. J. **526**, 215 (1999).
- [4] F. Donato *et al.*, Astrophys. J. **563**, 172 (2001).
- [5] V. S. Ptuskin *et al.*, Astrophys. J. **642**, 902 (2006).
- [6] S. Orito *et al.*, Phys. Rev. Lett. **84**, 1078 (2000).
- [7] O. Adriani *et al.*, Phys. Rev. Lett. **105**, 121101 (2010);
- [8] K. Sakai *et al.*, Proc. 32nd Int. Cosmic Ray Conf. (Beijing), (2011); K. Sakai, Ph. D Thesis, The University of Tokyo, (2011).
- [9] F. Donato *et al.*, Proc. 30th Int. Cosmic Ray Conf. (Merida), (2007).
- [10] P. Salati *et al.*, Particle Dark Matter: Observations, Models and Searches (Cambridge University Press), 521 (2010).
- [11] H. Fuke *et al.*, Phys. Rev. Lett. **95**, 081101 (2005);
- [12] J.W. Mitchell *et al.*, Proc. 31th Int. Cosmic Ray Conf. (Lodz), (2009).
- [13] V. Choutke *et al.*, Proc. 30th Int. Cosmic Ray Conf. (Merida) **4**, 765 (2007).
- [14] C.J. Hayley *et al.*, Adv. Spac. Res., (2011).
- [15] A. Yamamoto *et al.*, Adv. Spac. Res., (2011).
- [16] K. Yoshimura *et al.*, Proc. 31th Int. Cosmic Ray Conf. (Lodz), (2010).
- [17] K. Abe *et al.*, Phys. Lett. B **670**, 103 (2008).